

Proximity Effect in Systems of Parallel Conductors

Cite as: Journal of Applied Physics **43**, 2196 (1972); <https://doi.org/10.1063/1.1661474>

Submitted: 22 November 1971 . Published Online: 10 November 2003

Glenn S. Smith



View Online



Export Citation

ARTICLES YOU MAY BE INTERESTED IN

[Calculation of core loss and copper loss in amorphous/nanocrystalline core-based high-frequency transformer](#)

AIP Advances **6**, 055927 (2016); <https://doi.org/10.1063/1.4944398>

[Skin effect and proximity effect in multiconductor systems with applied currents and voltages](#)

Journal of Applied Physics **69**, 5035 (1991); <https://doi.org/10.1063/1.348168>

[Exact solution of the proximity effect equation by a splitting method](#)

Journal of Vacuum Science & Technology B: Microelectronics Processing and Phenomena **6**, 432 (1988); <https://doi.org/10.1116/1.583969>

Journal of
Applied Physics

SPECIAL TOPIC:
Polymer-Grafted Nanoparticles

Submit Today!

AIP
Publishing

⁴A. D. MacDonald and S. C. Brown, Phys. Rev. 75, 411 (1949).

⁵Handbook of Mathematical Functions with Formulas, Graphs, and Mathematical Tables, edited by M. Abramowitz and I. A.

Stegun, Natl. Bur. Std. (U.S. GPO, Washington, D.C., 1964), p. 504.

⁶C. K. Un, Ph.D. dissertation (University of Delaware, Newark, Del., 1969) (unpublished).

Proximity Effect in Systems of Parallel Conductors*

Glenn S. Smith

Gordon McKay Laboratory, Harvard University, Cambridge, Massachusetts 02138

(Received 22 November 1971)

A procedure is presented for determining the cross-sectional high-frequency current distribution and Ohmic resistance per unit length for systems of parallel round wires carrying equal currents. The additional Ohmic resistance due to the proximity effect is examined for various conductor spacings. An optimum spacing for minimum resistance is determined for systems of conductors with restricted dimensions. Theoretical current distributions are compared with measurements.

I. INTRODUCTION

Current interest in the accurate determination of the radiating efficiency of electrically small wire antennas has required a thorough investigation of the Ohmic resistance of closely spaced conductors. The geometry treated in this paper—systems of parallel in-line wires carrying equal currents—has Ohmic losses per unit length which are approximately the same as those in the parallel turns of an electrically small multiturn loop antenna.^{1,2}

In the system of parallel conductors the distribution of current over the conductor cross section is determined by the normal skin effect and a proximity effect. Both are manifestations of the same phenomenon, namely, eddy currents in the conductors. The former is usually considered to characterize the net current in a single conductor while the latter depends on the currents in neighboring conductors. At high frequencies, the skin effect causes a concentration of the current near the outside surfaces of a conductor. This is depicted in Fig. 1(a) for a single isolated round conductor. The current distribution on two parallel wires carrying equal codirectional currents is a result of both skin effect and proximity effect [see Fig. 1(b)]. The proximity effect forces the current to the outside edge of each conductor, much as the skin effect forces the current to the outside surface of the single conductor. For systems with several closely spaced conductors, the change in the current distribution due to the proximity effect can cause an increase in the Ohmic resistance of the conductors which is as large or larger than the skin effect resistance alone, i. e., larger than the Ohmic resistance of the isolated conductors.

The skin effect in round conductors is discussed in most texts on electromagnetic theory. The proximity effect has received much less attention. Most of the theoretical and experimental works on the proximity effect deal with two-wire systems where the wires carry equal currents in opposite directions.³⁻⁵ This geometry has a direct application to the problem of wave propagation along parallel wire transmission lines. The only investigations of the proximity effect in systems with more than two conductors appear to be those done in conjunc-

tion with determining Ohmic resistance and Q of inductance coils. Of the theoretical treatments, Butterworth's discussion of the alternating current resistance of cylindrical conductors and solenoidal coils is the most thorough.⁶ His work is considered the standard theoretical approach and is summarized in several places.⁷ The experimental work of Medhurst, however, indicates that Butterworth's calculations of the radio frequency resistance of coils are not valid over as large a range of parameters as expected; for certain dimensions, errors as large as 190% were observed.⁸

In this paper, systems composed of various numbers of in-line parallel conductors with dimensions specified in Fig. 2 are analyzed. All the conductors have the same circular cross section and carry equal currents in the same direction. Only the high-frequency case in which the currents are confined to a thin layer near the surface of the wires is considered.

II. HIGH-FREQUENCY FORM FOR CURRENT DISTRIBUTION

At sufficiently high frequencies, the skin depth d_s for a good conductor is a small quantity compared to the cross-sectional dimension and most of the current is confined to a thin layer near the surface. The magnetic field external to the conductor is approximately the same as the field of a perfect conductor of the same shape carrying an equivalent surface current. An expression for the time-average power loss per unit surface area of the good conductor in terms of the surface current K_s on the perfect conductor is

$$P \doteq \frac{1}{2} |R^s| |K_s|^2 \text{ W/m}^2, \quad (1)$$

where

$$R^s = 1/\sigma d_s \quad (2a)$$

is the surface resistance and

$$d_s = (2/\omega \mu_0 \sigma)^{1/2}. \quad (2b)$$

If the conductor is cylindrical and K_s is an axial current density, the power loss per unit length of the conductor is

$$P \doteq \frac{1}{2} R^s \oint |K_s|^2 dw \text{ W/m}, \quad (3)$$

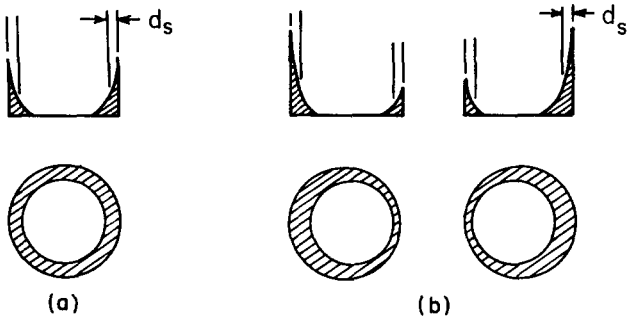


FIG. 1. (a) Skin effect in a single conductor. (b) Combination of skin effect and proximity effect in a system of two conductors. The shaded area represents the distribution of current on the surface of the wire.

where the integral is over the periphery of the conductor. For the isolated circular cylindrical conductor of radius a , rotational symmetry applies. Equation (3) reduces to the familiar "Rayleigh formula" for the high-frequency resistance per unit length of a circular conductor:

$$R_R = \frac{2P}{|I|^2} = \frac{R^s}{2\pi a} = \frac{1}{2\pi a} \left(\frac{\omega \mu_0}{2\sigma} \right)^{1/2} \Omega/\text{m}, \quad (4)$$

which is valid provided $a/d_s \gg 1$. With more than one conductor present, the current distribution and external fields for each conductor are no longer rotationally symmetric; therefore, (4) no longer applies. If the current distributions on the surface of the perfect conductors are sufficiently smooth, they can be represented by a finite number q of cosine Fourier series terms. On the m th conductor the current is

$$K_{sm}(\theta) = \frac{I_m}{2\pi a} g_m(\theta) = \frac{I_m}{2\pi a} \left(1 + \sum_{p=1}^q a_{mp} \cos(p\theta) \right), \quad (5)$$

where $g_m(\theta)$ is the normalized surface current density. From (3) the power loss per unit length for a good conductor expressed in terms of the coefficients a_{mp} for the perfect conductor becomes

$$P_m = \frac{I_m^2 R^s}{4\pi a} \left(1 + \frac{1}{2} \sum_{p=1}^q |a_{mp}|^2 \right) \text{W/m}. \quad (6)$$

A study of the complete expression for the current density in imperfectly conducting round wires indicates that (6), like (4), is only valid for small skin depths, specifically²

$$\frac{a}{d_s} \gg 1; \quad \frac{(pd_s/2a)^2}{1 - (p/2)^2(d_s/a)} \ll 1, \quad p = 1, 2, \dots, q. \quad (7)$$

The first term in (6) is the power loss in the m th conductor due to the net current I_m in that wire. This is the normal skin effect loss. The sum in (6) represents the loss due to nonuniform currents induced by other wires in the system. It is the additional loss in the m th wire due to the proximity effect. Since the coefficients a_{mp} in the sum are a function of the net currents I_m in all wires of the system, the equation for P_m cannot be written $P_m = R_m(\frac{1}{2}I_m^2)$, where R_m is only a function of the physical

parameters of the system. As a result, the usual circuit definition of the Ohmic resistance of each wire ($R_m = P_m/\frac{1}{2}I_m^2$) makes no sense.

When all conductors carry the same total current at each cross section, the Ohmic resistance per unit length of the system of wires is a useful quantity. For n parallel wires this is

$$R = \frac{R^s}{2\pi a} \sum_{m=1}^n \left(1 + \frac{1}{2} \sum_{p=1}^q |a_{mp}|^2 \right) \Omega/\text{m}. \quad (8)$$

Normalized quantities are useful when comparing different configurations of conductors. The normalized additional Ohmic resistance per unit length due to the proximity effect is

$$\frac{R_p}{R_0} = \frac{R - nR_R}{nR_R} = \frac{1}{2} \sum_{m=1}^n \sum_{p=1}^q |a_{mp}|^2 \Omega/\text{m}. \quad (9)$$

III. FORMULATION OF INTEGRAL EQUATIONS FOR TRANSVERSE CURRENT DISTRIBUTIONS

Consider each of the long parallel cylinders in Fig. 2 to be perfectly conducting. The surface current density on the l th conductor is then

$$K_l(\theta', z') = (I/2\pi a) g_l(\theta') f(z'), \quad l = 1, 2, \dots, n. \quad (10)$$

The dimensionless quantity $g_l(\theta')$ is the normalized surface current density. In (10) the same z' dependence $f(z')$ is assumed for the current distributions on all cyl-

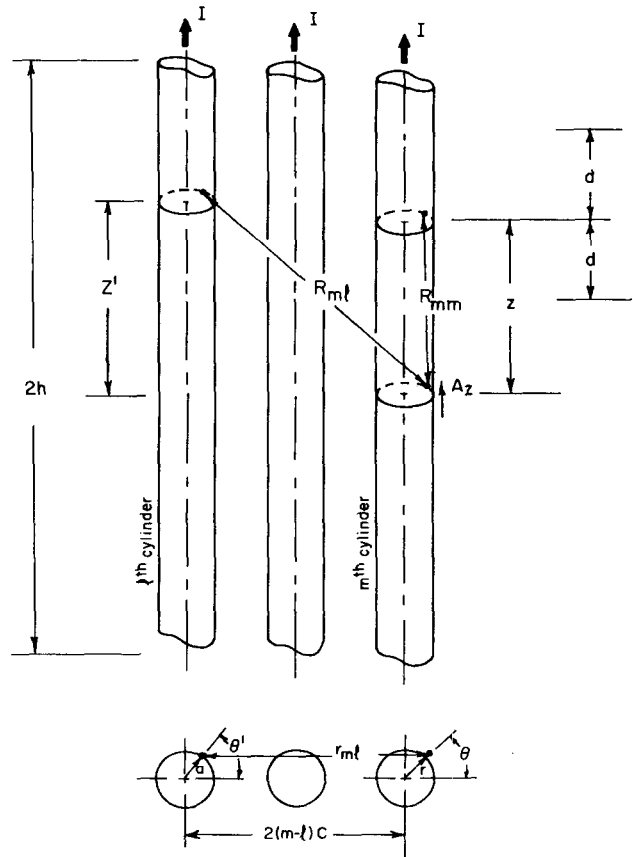


FIG. 2. Parallel wires of circular cross section carrying equal currents in the same direction.

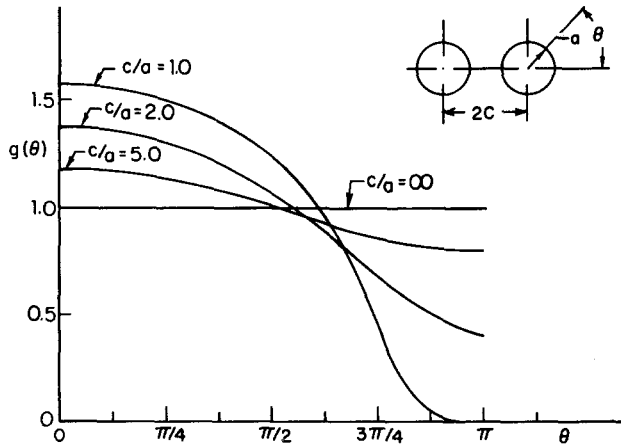


FIG. 3. Normalized surface current distribution on two wires for various wire spacings c/a .

inders. The conductors are composed of three sections: the length, $z - d \leq z' \leq z + d$, and the two end sections, $z + d \leq z' \leq h$, $-h \leq z' \leq z - d$. The following constraints are placed on the dimensions of the system:

$$\beta_0 d \ll 1, \quad a \ll d, \quad d^2 \gg n^2 c^2, \tag{11}$$

where β_0 is the free-space propagation constant. The current distribution at every cross section along the length $z - d \leq z' \leq z + d$ is then approximately the same:

$$K_I(\theta', z') \doteq (I/2\pi a) g_I(\theta') f(z), \quad z - d \leq z' \leq z + d. \tag{12}$$

The Helmholtz integral for the z component of the magnetic vector potential at a point (r, θ, z) just off the surface of the m th conductor is

$$\begin{aligned} A_{mz}(r, \theta, z) &= \frac{\mu_0 I}{8\pi^2} \left[f(z) \int_{z'-d}^{z'+d} \int_{\theta'=-\tau}^{\tau} \sum_{i=1}^n \left(\frac{g_i(\theta') e^{i\beta_0 R_{mi}}}{R_{mi}} \right) d\theta' dz' \right. \\ &\quad \left. + \left(\int_{z'=-h}^{z'-d} \int_{\theta'=-\tau}^{\tau} \sum_{i=1}^n \left(\frac{g_i(\theta') f(z') e^{i\beta_0 R_{mi}}}{R_{mi}} \right) d\theta' dz' \right) \right], \end{aligned} \tag{13}$$

where

$$\begin{aligned} R_{mi} &= [(z - z')^2 + r_{mi}^2]^{1/2} \\ &= [(z - z')^2 + 4(m-l)^2 c^2 + r^2 + a^2 - 2ar \cos(\theta - \theta') \\ &\quad + 4(m-l)c(r \cos \theta - a \cos \theta')]^{1/2}. \end{aligned} \tag{14}$$

An $e^{-i\omega t}$ time dependence is used. If terms of order $\beta_0 d$ or less are neglected in the first integral, and

$$R_{mi} \doteq [(z - z')^2 + 4(m-l)^2 c^2]^{1/2} \tag{15}$$

in the last two integrals, then (13) reduces to

$$\begin{aligned} A_{mz}(r, \theta, z) &\doteq \frac{\mu_0 I}{8\pi^2} \left[f(z) \int_{\theta'=-\tau}^{\tau} \sum_{i=1}^n \left(\frac{g_i(\theta')}{R_{mi}} \right) d\theta' dz' \right. \\ &\quad \left. + \left(\int_{z'=-h}^{z'-d} \int_{\theta'=-\tau}^{\tau} \right) 2\pi f(z') \right] \end{aligned}$$

$$\times \sum_{i=1}^n \left(\frac{\exp[i\beta_0 \{(z - z')^2 + 4(m-l)^2 c^2\}^{1/2}]}{[(z - z')^2 + 4(m-l)^2 c^2]^{1/2}} \right) dz' \tag{16}$$

The first integral can be evaluated directly. The result is

$$\begin{aligned} A_{mz}(r, \theta, z) &\doteq \frac{\mu_0 I}{8\pi^2} \left(-2f(z) \int_{\theta'=-\tau}^{\tau} \sum_{i=1}^n [g_i(\theta') \ln(r_{mi})] d\theta' \right. \\ &\quad \left. + 4\pi n \ln(2d) + A'_{mz}(z) \right). \end{aligned} \tag{17}$$

The term $A'_{mz}(z)$ represents the last two integrals in (16).

The normalized surface current density is given by the boundary condition

$$g_m(\theta) = - \frac{2\pi a}{\mu_0 I f(z)} \left. \frac{\partial A_{mz}(r, \theta, z)}{\partial r} \right|_{r=a}. \tag{18}$$

The next step is to substitute the approximate expression for the vector potential (17) into (18) to obtain

$$\begin{aligned} g_m(\theta) &\doteq \frac{1}{2\pi} \left(\lim_{\tau \rightarrow 1} \int_{\theta'=-\tau}^{\tau} \frac{g_m(\theta') [\tau - \cos(\theta - \theta')]}{\tau^2 + 1 - 2\tau \cos(\theta - \theta')} d\theta' \right. \\ &\quad \left. + \int_{\theta'=-\tau}^{\tau} \sum_{i=1, i \neq m}^n \frac{[1 + 2(m-l)(c/a) \cos \theta - \cos(\theta - \theta')] g_i(\theta')}{(r'_{mi})^2} d\theta' \right), \end{aligned} \tag{19}$$

where

$$\begin{aligned} \tau &= r/a, \\ r'_{mi} &= [4(m-l)^2 (c/a)^2 + 2 - 2 \cos(\theta - \theta') \\ &\quad + 4(m-l)(c/a)(\cos \theta - \cos \theta')]^{1/2}. \end{aligned} \tag{20}$$

The first integral, which represents the self-term, is indefinite when $\tau = 1$; therefore, the order of the limiting and integration processes are not interchangeable. For values of τ near unity the integrand has the behavior

$$\text{integrand} \sim \Delta / (\Delta^2 + \theta^2) + \frac{1}{2}, \quad \Delta = \tau - 1 \ll 1. \tag{21}$$

If this is compared with the following definition of the Dirac δ function

$$\delta(\theta) = \frac{1}{\pi} \lim_{\Delta \rightarrow 0} \frac{\Delta}{\Delta^2 + \theta^2}, \tag{22}$$

it is evident that in the limit the integrand becomes

$$\text{integrand} = \pi \delta(\theta) + \frac{1}{2}. \tag{23}$$

Substitution of (23) into (19) and subsequent rearrangement yield

$$g_m(\theta) = 1 + \frac{1}{\pi} \int_{\theta'=-\tau}^{\tau} \sum_{i=1, i \neq m}^n K_{m,i}(\theta, \theta') g_i(\theta') d\theta', \tag{24}$$

where

$$K_{m,i}(\theta, \theta') = [1 + 2(m-l)(c/a) \cos \theta - \cos(\theta - \theta')] / (r'_{mi})^2. \tag{25}$$

Symmetry about the center of the system of wires requires $g_{n+1-m}(\theta) = g_m(\pi - \theta)$, which reduces the number of terms in (24) to $\frac{1}{2}n$ for n even or $\frac{1}{2}(n+1)$ for n odd:

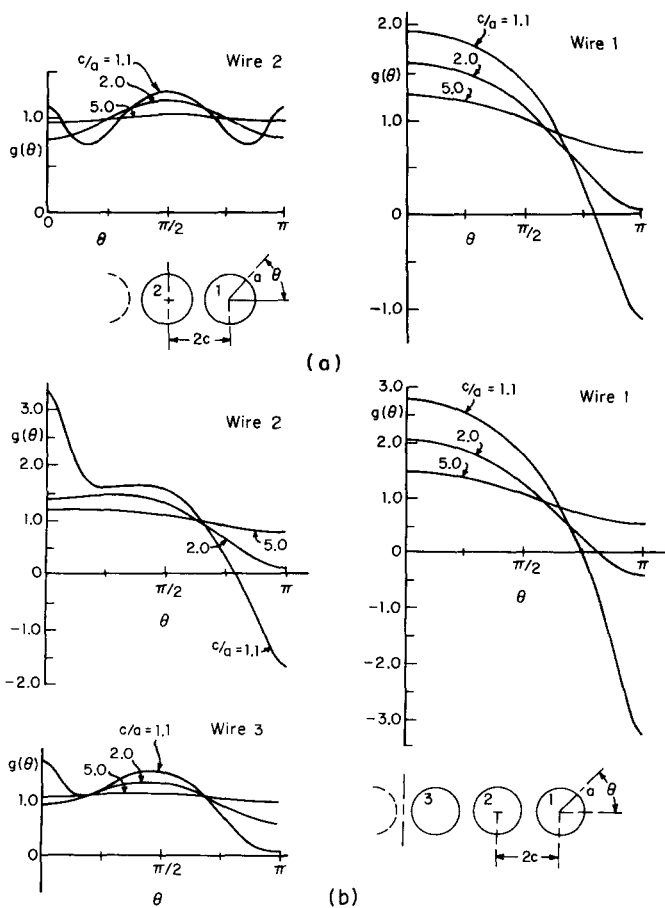


FIG. 4. Normalized surface current distributions for (a) three wires and (b) six wires.

n even:

$$g_m(\theta) = \frac{1}{\pi} \int_{\theta'=-\pi}^{\pi} K_{m,n+1-m}(\theta, \pi-\theta') g_m(\theta') d\theta' + \left(1 + \frac{1}{\pi} \sum_{\substack{i=1 \\ i \neq m}}^{n/2} [K_{m,i}(\theta, \theta') + K_{m,n+1-i}(\theta, \pi-\theta')] g_i(\theta') d\theta'\right), \quad (26a)$$

$m = 1, 2, \dots, \frac{1}{2}n;$

n odd:

$$g_m(\theta) = \frac{h(m)}{\pi} \int_{\theta'=-\pi}^{\pi} K_{m,n+1-m}(\theta, \pi-\theta') g_m(\theta') d\theta' + \left(1 + \frac{1}{\pi} \sum_{\substack{i=1 \\ i \neq m}}^{(n-1)/2} [K_{m,i}(\theta, \theta') + K_{m,n+1-i}(\theta, \pi-\theta')] g_i(\theta') d\theta'\right) + \frac{h(m)}{\pi} \int_{\theta'=-\pi}^{\pi} K_{m,(n+1)/2}(\theta, \theta') g_{(n+1)/2}(\theta') d\theta', \quad (26b)$$

$m = 1, 2, \dots, \frac{1}{2}(n+1),$

where

$$h(m) = 1, \quad m \neq \frac{1}{2}(n+1),$$

$$h(m) = 0, \quad m = \frac{1}{2}(n+1). \quad (27)$$

Equations (26a) and (26b) represent, respectively, a system of $\frac{1}{2}n$ and $\frac{1}{2}(n+1)$ coupled integral equations whose solutions are the desired surface current densities $g_m(\theta)$.

IV. SOLUTION FOR TWO CONDUCTORS

A problem in differential form equivalent to the integral formulation (26a) and (26b) involves the solution of the two-dimensional Laplace equation

$$\nabla^2 A_z = 0 \quad (28)$$

for the axial component of the vector potential in the region exterior to the conductors. The normalized surface current density is then determined from

$$g_m(\theta) = -\frac{2\pi a}{\mu_0 I} \left. \frac{\partial A_z}{\partial r_m} \right|_{r_m=a}, \quad (29)$$

where r_m is the radial distance from the center of the m th cylinder. This problem is mathematically identical to the electrostatic case in which the wires carry equal charges rather than currents. The electrostatic problem for two circular conductors was first solved by Whipple using a conformal mapping technique.⁹ In the context of the present problem the solution is¹

$$g(\theta) = \frac{2(1+k)K(k)}{\pi} \operatorname{csch} \alpha (\cosh \alpha - \cos u) \times dn \left(\frac{(1+k)K(k)}{\pi} u, \frac{2\sqrt{k}}{1+k} \right), \quad (30a)$$

with

$$u = \sin^{-1} \left(\frac{\sin \theta \sinh \alpha}{c/a + \cos \theta} \right), \quad \alpha = \ln \left(\frac{a}{c - (c^2 - a^2)^{1/2}} \right), \quad (30b)$$

$$\frac{K'(k)}{K(k)} = 2\alpha/\pi;$$

dn is a Jacobi elliptic function and $K(k)$ and $iK'(k)$ are the real and imaginary quarter-periods of the elliptic function. Figure 3 is a graph of the normalized current distribution for various wire spacings c/a . The aforementioned crowding of the current near the outside edges of the wires due to the proximity effect is evident. The normalized additional Ohmic resistance per unit length due to the proximity effect is

$$\frac{R_p}{R_0} = \left(\frac{2K}{\pi} \right)^2 \left[2 \operatorname{ctnh} \alpha \left(\frac{E(K, k)}{K} - \frac{k'^2}{2} \right) \right] - (1 + 2 \operatorname{csch}^2 \alpha), \quad (31)$$

where $E(K, k)$ is the complete elliptic integral of the second kind and $k'^2 = 1 - k^2$.

V. APPROXIMATE SOLUTION OF INTEGRAL EQUATIONS FOR TWO OR MORE CONDUCTORS

For systems with more than two circular conductors a solution in closed form like (30a) for the two-wire case is unavailable. Approximate methods must be used to obtain the current distribution and resulting Ohmic resistance per unit length of the system. In this section one such method, undetermined coefficients, is applied to the previously derived system of integral equations

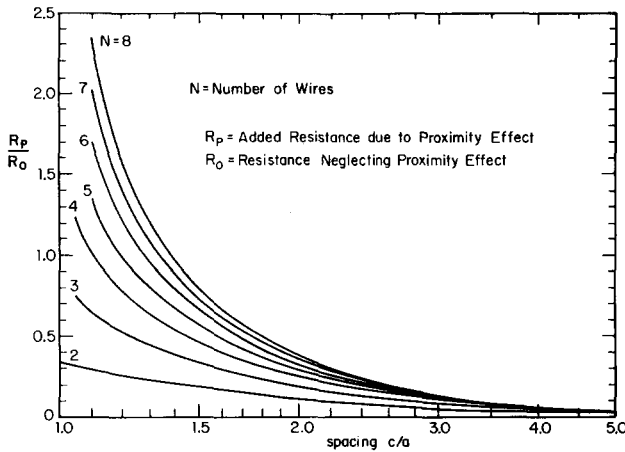


FIG. 5. Additional Ohmic resistance per unit length of a system of parallel wires due to the proximity effect.

(26a) and (26b). As suggested in Sec. II, a trigonometric series is the natural choice for an expansion to represent the normalized surface current density:

$$g_m(\theta) = 1 + \sum_{p=1}^q a_{mp} \cos(p\theta). \tag{32}$$

Further evidence for this selection is found by examining the exact solution for two wires. A Fourier series analysis of the current distribution (30a) for the limiting case $c/a=1$ indicates that the first two cosine terms in the series are adequate to predict the additional loss due to proximity R_p/R_0 to within 1%. For large spacings, $c/a \gg 1$, the current distribution is of the form $1 + a \cos \theta$ as seen in Fig. 3. This last statement is also true for systems with more than two wires and is easily understood if the magnetic field due to external currents is considered as constant over the cross section of each conductor. The magnetic field B_{my} normal to the axis of the m th conductor in a system of n conductors would be

$$B_{my} = \frac{\mu_0 I}{4\pi c} \sum_{\substack{l=1 \\ l \neq m}}^n \frac{1}{m-l}. \tag{33}$$

The resulting current distribution becomes

$$g_m(\theta) = 1 + \left(\frac{a}{c} \sum_{\substack{l=1 \\ l \neq m}}^n \frac{1}{m-l} \right) \cos \theta. \tag{34}$$

Now, the substitution of (32) for $g_m(\theta)$ in (26a) and (26b) yields

n even:

$$\begin{aligned} & \sum_{p=1}^q a_{mp} \left(-\cos(p\theta) + \frac{(-1)^p}{\pi} \int_{\theta'=-\tau}^{\tau} K_{m,n+1-m}(\theta, \theta') \cos(p\theta') d\theta' \right) \\ & + \sum_{\substack{l=1 \\ l \neq m}}^{n/2} \sum_{p=1}^q a_{lp} \left(\frac{1}{\pi} \int_{\theta'=-\tau}^{\tau} [K_{m,l}(\theta, \theta') + (-1)^p K_{m,n+1-l}(\theta, \theta')] \right. \\ & \left. \times \cos(p\theta') d\theta' \right) \\ & = \frac{-1}{\pi} \int_{\theta'=-\tau}^{\tau} \left(K_{m,n+1-m}(\theta, \theta') + \sum_{\substack{l=1 \\ l \neq m}}^{n/2} [K_{m,l}(\theta, \theta')] \right. \end{aligned}$$

$$\left. + K_{m,n+1-l}(\theta, \theta') \right) d\theta', \tag{35}$$

$m = 1, 2, \dots, \frac{1}{2}n,$

where the same number of harmonic terms q is used to represent the surface current on all conductors. For the sake of brevity, only the n even case is examined. The definite integrals in (35) are of the form

$$\begin{aligned} I(\theta, m-l, p) &= (1/\pi) \int_{\theta'=-\tau}^{\tau} [1 + 2(m-l)(c/a)\cos\theta \\ & - (\cos\theta \cos\theta' + \sin\theta \sin\theta')] \cos(p\theta') d\theta' \\ & \times \{4(m-l)^2(c/a)^2 + 2 + 4(m-l)(c/a)\cos\theta \\ & - [4(m-l)(c/a) + 2\cos\theta'] \cos\theta' \\ & - 2\sin\theta \sin\theta'\}^{-1}. \end{aligned} \tag{36}$$

An exact evaluation of this integral yields

$$\begin{aligned} I(\theta, m-l, p) &= \frac{1}{(1-s^2)(-s)^{p+1}} (As^2 + Bs + C), \\ & p = 1, 2, \dots, q \\ & = \frac{-1}{s(1-s^2)} (Bs + C), \quad p = 0, \end{aligned} \tag{37a}$$

where

$$s = [4(m-l)^2(c/a)^2 + 1 + 4(m-l)(c/a)\cos\theta]^{1/2}, \tag{37b}$$

$$A = \cos[\theta - (p-1)\psi], \tag{37c}$$

$$B = 2[1 + 2(m-l)(c/a)\cos\theta] \cos(p\psi), \tag{37d}$$

$$C = \cos[\theta + (p+1)\psi], \tag{37e}$$

$$\begin{aligned} \psi &= \pi - \tan^{-1} \left(\frac{\sin\theta}{2(m-l)(c/a) + \cos\theta} \right), \quad m-l = 1, 2, \dots, \\ & = \tan^{-1} \left(\frac{-\sin\theta}{2(m-l)(c/a) + \cos\theta} \right), \quad m-l = -1, -2, \dots \end{aligned} \tag{37f}$$

With this notation (35) becomes

TABLE I. Normalized additional Ohmic resistance per unit length due to the proximity effect R_p/R_0 .

c/a	Numbers of conductors						
	2	3	4	5	6	7	8
1.00	0.333						
1.05	0.316	0.743	1.231				
1.10	0.299	0.643	0.996	1.347	1.689	2.020	2.340
1.15	0.284	0.580	0.868	1.142	1.400	1.643	1.872
1.20	0.268	0.531	0.777	1.002	1.210	1.401	1.577
1.25	0.254	0.491	0.704	0.896	1.068	1.224	1.365
1.30	0.240	0.455	0.644	0.809	0.956	1.086	1.203
1.40	0.214	0.395	0.546	0.674	0.784	0.880	0.965
1.50	0.191	0.346	0.470	0.572	0.658	0.732	0.796
1.60	0.173	0.305	0.408	0.492	0.561	0.620	0.670
1.70	0.155	0.270	0.358	0.428	0.485	0.532	0.573
1.80	0.141	0.241	0.316	0.375	0.423	0.462	0.495
1.90	0.128	0.216	0.281	0.332	0.372	0.405	0.433
2.00	0.116	0.195	0.252	0.295	0.330	0.358	0.382
2.20	0.098	0.161	0.205	0.239	0.265	0.286	0.304
2.40	0.082	0.135	0.170	0.197	0.217	0.234	0.247
2.50	0.077	0.124	0.156	0.180	0.198	0.213	0.225
2.60	0.071	0.114	0.144	0.165	0.182	0.195	0.206
2.80	0.061	0.098	0.123	0.141	0.154	0.165	0.174
3.00	0.054	0.085	0.106	0.121	0.133	0.142	0.150
3.50	0.040	0.062	0.077	0.087	0.095	0.101	0.106
4.00	0.031	0.048	0.058	0.066	0.072	0.076	0.080

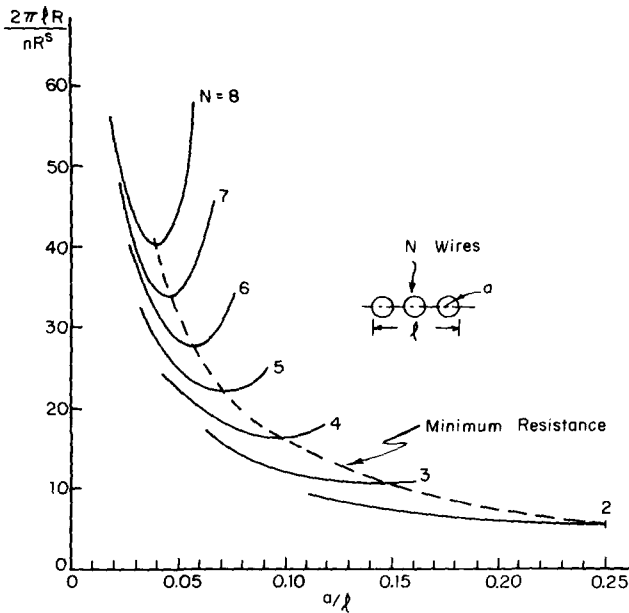


FIG. 6. Ohmic resistance as a function of the wire radius a with the depth of winding l fixed.

$$\sum_{p=1}^q a_{mp} [-\cos(p\theta) + (-1)^p I(\theta, 2m-n-1, p)] + \sum_{\substack{i=1 \\ i \neq m}}^{n/2} \sum_{p=1}^q a_{ip} [I(\theta, m-l, p) + (-1)^p I(\theta, m+l-n-1, p)] = - \left(I(\theta, 2m-n-1, 0) + \sum_{\substack{i=1 \\ i \neq m}}^{n/2} [I(\theta, m-l, 0) + I(\theta, m+l-n-1, 0)] \right), \quad m=1, 2, \dots, \frac{1}{2}n. \quad (38)$$

This is a set of $\frac{1}{2}n$ equations, one for each conductor, involving $\frac{1}{2}qn$ unknowns (a_{mp}), the coefficients of which are functions of the variable θ . In order to solve the system, a set of $\frac{1}{2}qn$ conditions is necessary. One procedure which yields such conditions is the method of least squares in which the a_{mp} are chosen in a manner such that (38) is satisfied in a least-squares sense over the interval $0 \leq \theta \leq \pi$; thus,¹⁰

$$\int_{\theta=0}^{\pi} \left(\sum_{p=1}^q a_{mp} [-\cos(p\theta) + (-1)^p I(\theta, 2m-n-1, p)] + \sum_{\substack{i=1 \\ i \neq m}}^{n/2} \sum_{p=1}^q a_{ip} [I(\theta, m-l, p) + (-1)^p I(\theta, m+l-n-1, p)] + I(\theta, 2m-n-1, 0) + \sum_{\substack{i=1 \\ i \neq m}}^{n/2} [I(\theta, m-l, 0) + I(\theta, m+l-n-1, 0)] \right)^2 d\theta = \text{minimum}, \quad m=1, 2, \dots, \frac{1}{2}n. \quad (39)$$

When the left-hand side of (39) is differentiated with respect to each coefficient a_{mp} and the results are set equal to zero, the result is

$$\sum_{p=1}^q a_{mp} \left((\pi/2) \delta(k-p) - \int_{\theta=0}^{\pi} [(-1)^p \cos(k\theta) I(\theta, 2m-n-1, p) + (-1)^k \cos(p\theta) I(\theta, 2m-n-1, k) - (-1)^{p+k} I(\theta, 2m-n-1, p) I(\theta, 2m-n-1, k)] d\theta \right) + \sum_{\substack{i=1 \\ i \neq m}}^{n/2} \sum_{p=1}^q a_{ip} \left(- \int_{\theta=0}^{\pi} [\cos(k\theta) - (-1)^k I(\theta, 2m-n-1, k)] \times [I(\theta, m-l, p) + (-1)^p I(\theta, m+l-n-1, p)] d\theta \right) = \int_{\theta=0}^{\pi} [\cos(k\theta) - (-1)^k I(\theta, 2m-n-1, k)] \times \left(I(\theta, 2m-n-1, 0) + \sum_{\substack{i=1 \\ i \neq m}}^{n/2} [I(\theta, m-l, 0) + I(\theta, m+l-n-1, 0)] \right) d\theta, \quad (40)$$

which can be written

$$\sum_{p=1}^q a_{mp} t_{kp}^m + \sum_{\substack{i=1 \\ i \neq m}}^{n/2} a_{ip} t_{kp}^{im} = s_{mk}, \quad m=1, 2, \dots, \frac{1}{2}n, \quad k=1, 2, \dots, q. \quad (41)$$

In matrix form, the system of algebraic equations (40) is now

$$\begin{bmatrix} T_{11} & T_{12} & \dots & T_{1, n/2} \\ T_{21} & T_{22} & \dots & T_{2, n/2} \\ \vdots & \vdots & \ddots & \vdots \\ T_{n/2, 1} & T_{n/2, 2} & \dots & T_{n/2, n/2} \end{bmatrix} \begin{bmatrix} A_1 \\ A_2 \\ \vdots \\ A_{n/2} \end{bmatrix} = \begin{bmatrix} S_1 \\ S_2 \\ \vdots \\ S_{n/2} \end{bmatrix}, \quad (42a)$$

where

$$T_{ii} = \begin{bmatrix} t_{11}^i & t_{12}^i & \dots & t_{1q}^i \\ t_{21}^i & t_{22}^i & \dots & t_{2q}^i \\ \vdots & \vdots & \ddots & \vdots \\ t_{q1}^i & t_{q2}^i & \dots & t_{qq}^i \end{bmatrix}, \quad T_{ij} = \begin{bmatrix} t_{11}^{ij} & t_{12}^{ij} & \dots & t_{1q}^{ij} \\ t_{21}^{ij} & t_{22}^{ij} & \dots & t_{2q}^{ij} \\ \vdots & \vdots & \ddots & \vdots \\ t_{q1}^{ij} & t_{q2}^{ij} & \dots & t_{qq}^{ij} \end{bmatrix}, \quad (42b)$$

TABLE II. Conductor spacings for minimum resistance.

Number of conductors n	a/l	c/a	$2\pi lR/R^2$
2	0.250	1.00	5.33
3	0.148	1.19	10.41
4	0.098	1.37	16.07
5	0.071	1.50	22.01
6	0.056	1.59	28.10
7	0.046	1.66	34.30
8	0.039	1.71	40.57

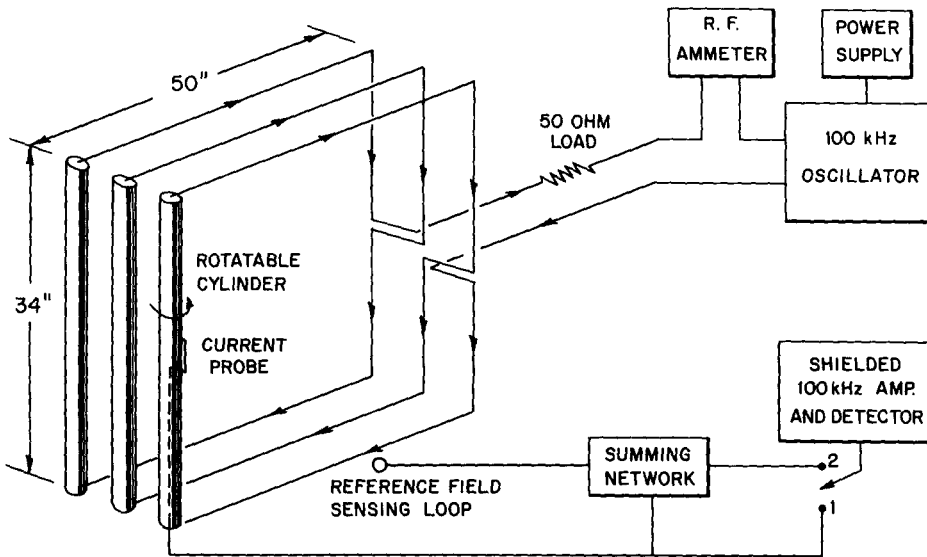


FIG. 7. Block diagram of the current-measuring equipment.

$$A_t = \begin{bmatrix} a_{t1} \\ a_{t2} \\ \vdots \\ a_{tq} \end{bmatrix}, \quad S_t = \begin{bmatrix} s_{t1} \\ s_{t2} \\ \vdots \\ s_{tq} \end{bmatrix}. \quad (42c)$$

The definite integrals that appear in the elements of the T and S matrices were performed numerically and the resulting matrix equation (42a) was solved for the coefficients a_{mp} .

The number of harmonic terms used for the current distribution on a given system of conductors was determined by observing the normalized resistance R_p/R_0 . If increasing the number by two produced less than a 0.10% change in R_p/R_0 , the number of terms was deemed sufficient. The normalized surface current densities $g(\theta)$ for systems with 3 and 6 conductors with various spacings (c/a) are plotted in Fig. 4. Note that there are both positive and negative currents on the surface of the outer conductors when the conductors are closely spaced. These currents in opposite directions add nothing to the net current in the wires; they just increase the Ohmic loss. In Fig. 5 and Table I, the additional Ohmic resistance due to the proximity effect (9) is plotted against the conductor spacing (c/a) for systems with up to 8 conductors. The proximity effect is an important factor in determining the resistance; for close conductor spacings it can increase the resistance by an amount as large or larger than the skin effect resistance of the isolated conductors. The curves presented in Fig. 5 were all obtained using six or fewer harmonic terms in the series for $g(\theta)$. These results will be valid for conductors with parameters which satisfy the following inequalities [from (7)]:

$$\frac{a}{d_s} \gg 1, \quad \frac{9(d_s/a)^2}{1 - 9(d_s/a)^2} \ll 1. \quad (43)$$

These conditions are met by most wire sizes used in practical antennas operating at frequencies above 1 MHz.

In certain applications a given number n of parallel in-line conductors must fit within a specified length l (see Fig. 6). It is of interest to ask for which wire radius a , or spacing c/a , the resistance of the wires is a minimum. If there were no proximity effect, the skin effect resistance would be minimized with as large a radius of the wire as possible ($a \approx l/2n$). With the proximity effect present, increasing the wire radius increases the loss

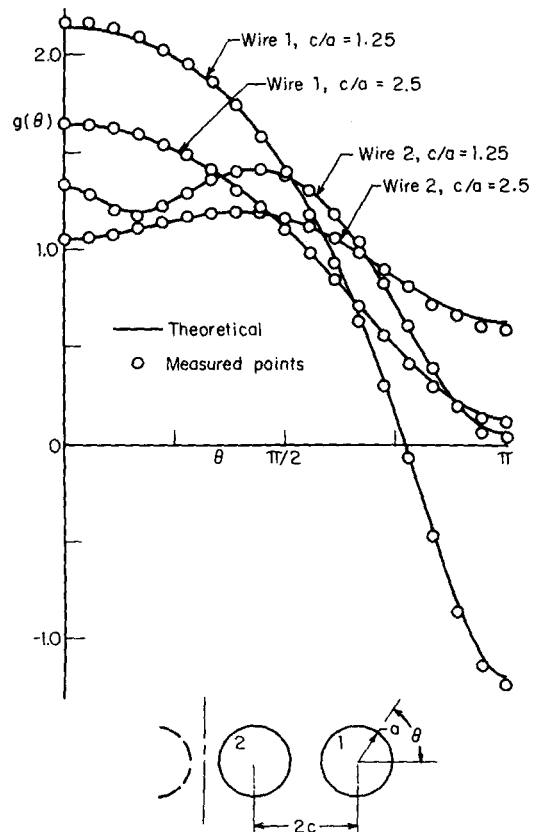


FIG. 8. Measured and theoretical surface current distributions for four wires.

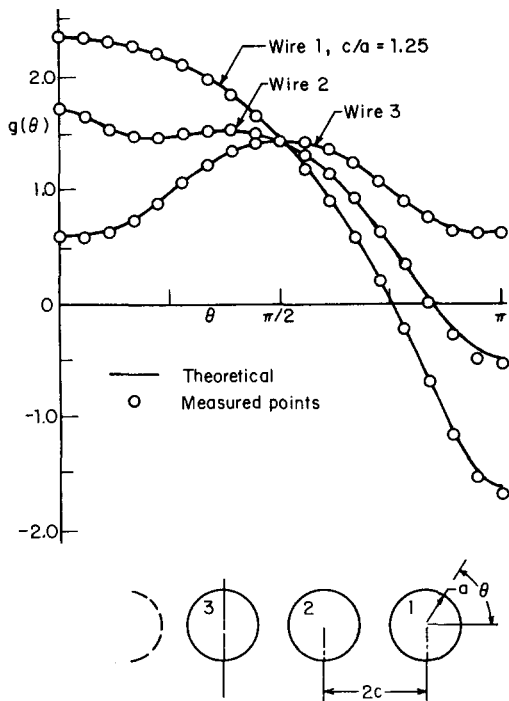


FIG. 9. Measured and theoretical surface current distributions for five wires.

due to proximity and a minimum resistance point is reached where the decrease in skin effect loss is just balanced by an increase in proximity loss. In Fig. 6 the dimensionless quantity $2\pi lR/\pi R^2$, which is proportional to the total Ohmic resistance per unit length of the system of conductors, is plotted against the normalized wire radius a/l . The points of minimum resistance are clearly exhibited in Fig. 6 and the corresponding conductor spacings are listed in Table II.

VI. EXPERIMENTAL INVESTIGATION

Apparatus was constructed for measuring the transverse distribution of current on a system of parallel round wires. The wires were modeled by long copper tubes interconnected with wire braids to carry equal currents in the same direction (see Fig. 7). The current distribution was measured by sampling the transverse magnetic field with a small loop probe mounted on one of the tubes. This tube was interchangeable with the other tubes in the system. At 100 kHz the $1\frac{1}{4}$ -in. copper pipes are about 200 skin depths in diameter and 20 skin depths thick; thus, they are a good approximation to solid conductors with axial currents confined to a thin layer near the outside surface. A full description of the apparatus and experimental procedures is given elsewhere.²

Theoretical and measured current distributions are given in Figs. 8 and 9 for four- and five-wire systems with various spacings (c/a). Agreement between theory and experiment is seen to be very good.

VII. CONCLUSION

Systems of equally spaced in-line conductors carrying equal currents in the same direction have been studied. A set of integral equations was formulated to determine the transverse distribution of axial current at high frequencies when the current is confined to a thin skin near the surface of the conductor. An approximate solution of the integral equations for the current was obtained in the form of a trigonometric series. For two wires the approximate solution for the current showed good agreement with an exact expression obtained by a conformal mapping procedure. With the current distribution determined, the high-frequency resistance per unit length of the system was calculated for various numbers of conductors and spacings.

Only cylinders carrying equal currents in the same direction were considered. With a simple scaling of harmonic terms on each conductor the present theory could handle systems of wires with different currents in each wire. Such a solution would be useful for making computations for multiwire transmission lines where the wires carry currents with equal magnitude but in opposite directions.

ACKNOWLEDGMENTS

The author wishes to thank Professor R. W. P. King and Dr. L. D. Scott for their helpful discussions on this problem. In addition, the author is very grateful to V. Richard for bringing this problem to his attention.

*Research partially supported by the Microwave Physics Branch, Ballistic Research Laboratories, U.S. Army Aberdeen Proving Ground, under Joint Services Electronics Program, Contract No. N00014-67-A-0298-0005.

¹G. Smith, Division of Engineering and Applied Physics, Harvard University, Technical Report No. 612 (1970) (unpublished).

²G. Smith, Division of Engineering and Applied Physics, Harvard University, Technical Report No. 624 (1971) (unpublished).

³J. R. Carson, *Phil. Mag.* 41, 607 (1921).

⁴H. B. Dwight, *Trans. AIEE* 42, 850 (1923).

⁵A. E. Kennelly and H. A. Affel, *Proc. IRE* 4, 523 (1916).

⁶S. Butterworth, *Expt. Wireless Engr.* 3, 203 (1926); 3, 309 (1926); 3, 417 (1926); 3, 483 (1926).

⁷F. E. Terman, *Radio Engineers Handbook* (McGraw-Hill, New York, 1943), pp. 74-83.

⁸R. G. Medhurst, *Expt. Wireless Engr.* 24, 281, 35 (1946); 24, 282, 80 (1947).

⁹F. J. W. Whipple, *Proc. Roy. Soc. (London) A* 96, 465 (1920).

¹⁰F. B. Hildebrand, *Methods of Applied Mathematics* (Prentice-Hall, Englewood Cliffs, N.J., 1952), Chap. 4, Secs. 4.16-4.19.